

# Multi-gap nodeless superconductivity in iron selenide $\text{FeSe}_x$ : evident from quasiparticle heat transport

J. K. Dong,<sup>1</sup> T. Y. Guan,<sup>1</sup> S. Y. Zhou,<sup>1</sup> X. Qiu,<sup>1</sup>

L. Ding,<sup>1</sup> C. Zhang,<sup>1</sup> U. Patel,<sup>2</sup> Z. L. Xiao,<sup>2</sup> S. Y. Li<sup>1,\*</sup>

<sup>1</sup>*Department of Physics, Surface Physics Laboratory (National Key Laboratory),  
and Laboratory of Advanced Materials, Fudan University, Shanghai 200433, P. R. China*

<sup>2</sup>*Department of Physics, Northern Illinois University, DeKalb, Illinois 60115, USA*

(Dated: June 21, 2009)

The in-plane thermal conductivity  $\kappa$  of the iron selenide superconductor  $\text{FeSe}_x$  ( $T_c = 8.8$  K) were measured down to 120 mK and up to 14.5 T ( $\simeq 3/4 H_{c2}$ ). In zero field, the residual linear term  $\kappa_0/T$  at  $T \rightarrow 0$  is only about  $16 \mu\text{W K}^{-2} \text{cm}^{-1}$ , less than 4% of its normal state value. Such a small  $\kappa_0/T$  does not support the existence of nodes in the superconducting gap. More importantly, the field dependence of  $\kappa_0/T$  in  $\text{FeSe}_x$  is very similar to that in  $\text{NbSe}_2$ , a typical multi-gap  $s$ -wave superconductor. We consider our data as strong evidence for multi-gap nodeless superconductivity in  $\text{FeSe}_x$ . This kind of superconducting gap structure may be generic for all Fe-based superconductors.

PACS numbers: 74.25.Fy, 74.25.Op, 74.25.Jb

Just as CuO-plane is the basic building block of high- $T_c$  cuprate superconductors, the FeAs-layer is the basic structure of the newly discovered FeAs-based high- $T_c$  superconductors.<sup>1,2,3,4,5,6,7</sup> The FeAs-layer consists of a Fe square planar sheet tetrahedrally coordinated by As. However, unlike the rigid CuO-plane in cuprates, partial substitution of Fe by Co or Ni, or As by P within the FeAs-layer can effectively induce superconductivity.<sup>8,9,10,11,12</sup> In this sense, the discovery of superconductivity in binary  $\text{FeSe}_x$  ( $T_c \simeq 8$  K) is of great interests, since it only contains the superconducting FeSe-layer which has identical structure as FeAs-layer, and the Se deficiency may cause the superconductivity.<sup>13</sup> More remarkably, the onset  $T_c$  can be enhanced to as high as 37 K for  $\text{FeSe}_x$  under high pressure,<sup>14,15,16</sup> which further implies that superconductivity in  $\text{FeSe}_x$  may have the same mechanism as in FeAs-based superconductors.

For this new family of high- $T_c$  superconductors, the pairing symmetry of its superconducting gap is a key to understand the mechanism of superconductivity. Extensive experimental and theoretical work have been done to address this important issue for FeAs-based superconductors (for a theoretical review, see Ref. 17; for an experimental review, see Ref. 18). Although there is still no consensus, more and more evidences point to multi-gap nodeless superconductivity, possibly an unconventional  $s^\pm$  pairing mediated by antiferromagnetic fluctuations.<sup>19</sup> For the prototype  $\text{FeSe}_x$  superconductor, however, there were very few experiments to study the superconducting gap structure. This is due to its relatively lower  $T_c$  and lack of sizable high-quality single crystals.<sup>20,21</sup> The measurements of in-plane magnetic penetration depth for polycrystal  $\text{FeSe}_{0.85}$  are in favor of anisotropic  $s$ -wave superconducting gap or two gaps ( $s + s$ ).<sup>22</sup> To clarify this important issue, more experimental work are needed for  $\text{FeSe}_x$  superconductor.

Low-temperature thermal conductivity measurement is a powerful tool to study the superconducting gap structure.<sup>23</sup> The field dependence of the residual thermal

conductivity  $\kappa_0/T$  for  $\text{BaNi}_2\text{As}_2$  ( $T_c = 0.7$  K) is consistent with a dirty fully gapped superconductivity.<sup>24</sup> For  $\text{Ba}_{1-x}\text{K}_x\text{Fe}_2\text{As}_2$  ( $T_c \simeq 30$  K) and  $\text{BaFe}_{1.9}\text{Ni}_{0.1}\text{As}_2$  ( $T_c = 20.3$  K), a negligible  $\kappa_0/T$  was found in zero field, indicating a full superconducting gap.<sup>25,26</sup> However,  $\kappa(T)$  was only measured in magnetic fields up to  $H = 15$  T ( $\simeq 1/4 H_{c2}$ ), thus can not show clearly whether the superconductivity has multi-gap character in FeAs-based superconductors.<sup>25,26</sup>

In this paper, we measure the thermal conductivity  $\kappa$  of a  $\text{FeSe}_x$  single crystal with  $T_c = 8.8$  K down to 120 mK and up to 14.5 T ( $\simeq 3/4 H_{c2}$ ) to probe its superconducting gap structure. In zero field,  $\kappa_0/T$  is about  $16 \mu\text{W} / \text{K}^2 \text{cm}$ , less than 4% of its normal-state value. Such a small  $\kappa_0/T$  should not come from the nodal quasiparticle contribution. It may simply come from the slight overestimation when doing extrapolation, due to the lack of lower temperature data. The field-dependence of  $\kappa_0/T$  is very similar to that in multi-gap  $s$ -wave superconductor  $\text{NbSe}_2$ . Based on our data, it is evident that  $\text{FeSe}_x$  is a multi-gap nodeless superconductor.

$\text{FeSe}_x$  single crystals with nominal formula  $\text{FeSe}_{0.82}$  were grown via a vapor self-transport method.<sup>21</sup> The  $ab$ -plane dimensions of as-grown crystals ranges from a few hundred  $\mu\text{m}$  to 1 mm. Energy Dispersive of X-ray (EDX) microanalysis (Hitachi S-4800) show that the actual Fe:Se ratio is very close to 1:1 in our  $\text{FeSe}_x$  single crystals. The nominal formula  $\text{FeSe}_{0.82}$  was used in the initial work by Hsu et al.<sup>13</sup> However, the actual superconducting phase was later determined to be  $\text{FeSe}_{0.99 \pm 0.02}$  in Ref. 27 and  $\text{FeSe}_{0.974 \pm 0.005}$  in Ref. 28. Therefore the EDX result of our  $\text{FeSe}_x$  single crystals is consistent with these two later reports.

The ac magnetization was measured in a Quantum Design Physical Property Measurement System (PPMS). An as-grown single crystal with dimensions  $1.0 \times 0.40 \text{ mm}^2$  in the plane and  $190 \mu\text{m}$  thickness along the  $c$ -axis was selected for transport study. Contacts were made directly on the sample surfaces with silver paint, which

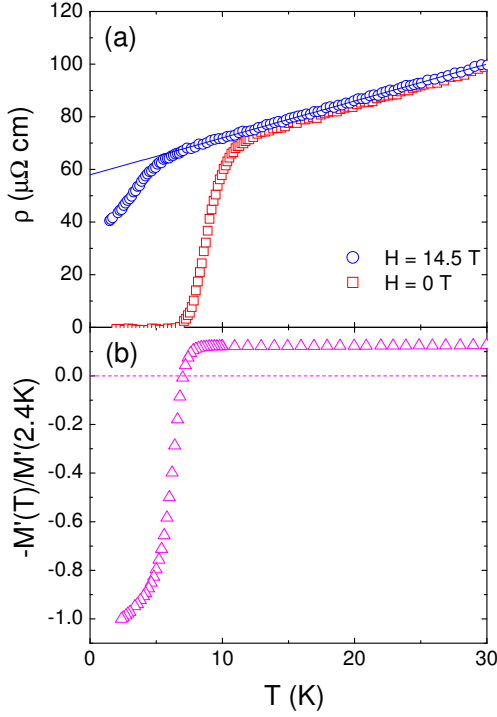


FIG. 1: (Color online) (a) In-plane resistivity  $\rho(T)$  of  $\text{FeSe}_x$  single crystal in  $H = 0$  and  $14.5 \text{ T}$  magnetic fields along the  $c$ -axis. The solid line is a linear fit of  $\rho(T)$  from 8 to 30 K, which gives the residual resistivity  $\rho_0 = 57.9 \mu\Omega \text{ cm}$  in  $H = 14.5 \text{ T}$ . (b) Normalized ac magnetization.

were used for both resistivity and thermal conductivity measurements. The typical contact resistance is a few ohms at room temperature and 1.5 K, which is not as good as that on  $\text{Ba}_{1-x}\text{K}_x\text{Fe}_2\text{As}_2$  and  $\text{BaFe}_{1.9}\text{Ni}_{0.1}\text{As}_2$  single crystals.<sup>25,26</sup> In-plane thermal conductivity was measured in a dilution refrigerator using a standard one-heater-two-thermometer steady-state technique. Due to the small size of the sample and the non-ideal contacts, good thermalization between sample and the two  $\text{RuO}_2$  thermometers can only be achieved down to 120 mK. Magnetic fields were applied along the  $c$ -axis and perpendicular to the heat current. To ensure a homogeneous field distribution in the sample, all fields were applied at temperature above  $T_c$ .

Fig. 1a shows the in-plane resistivity of  $\text{FeSe}_x$  single crystal in  $H = 0$  and  $14.5 \text{ T}$  magnetic fields. The middle point of the resistive transition is at  $T_c = 8.8 \text{ K}$  in zero field. The 10-90% transition width of our crystal is as broad as the powder sample,<sup>13</sup> which has been noticed in Ref. 21. Above  $T_c$ ,  $\rho(T)$  manifests a very good linear dependence up to 80 K, similar to the powder sample.<sup>13</sup> A linear fit of  $\rho(T)$  gives the residual resistivity  $\rho_0 = 57.9 \mu\Omega \text{ cm}$  in  $H = 14.5 \text{ T}$ , which is about 1/4 the value of powder sample.<sup>13</sup>

To estimate the upper critical field  $H_{c2}(0)$  which completely suppresses the resistive transition, we define  $T_c(\text{onset})$  at the temperature where  $\rho(T)$  deviates from

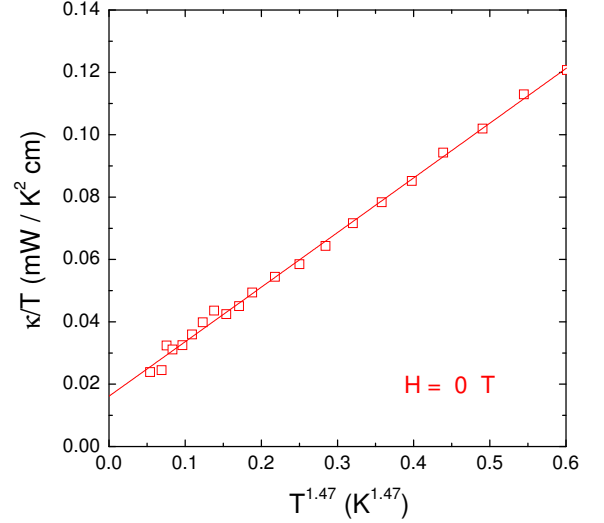


FIG. 2: (Color online) Temperature dependence of the in-plane thermal conductivity for  $\text{FeSe}_x$  single crystal in zero field. The solid line represents a fit of the data to  $\kappa/T = a + bT^{\alpha-1}$ . This gives the residual linear term  $\kappa_0/T = 16 \pm 2 \mu\text{W K}^{-2} \text{ cm}^{-1}$ .

the linear dependence, and get  $T_c(\text{onset}) = 11.9$  and  $6.3 \text{ K}$  for  $H = 0$  and  $14.5 \text{ T}$ , respectively. Using the relationship  $H_{c2}/H_{c2}(0) = 1 - (T_c/T_c(0))^2$ , we get  $H_{c2}(0) = 20.1 \text{ T}$ . Note that  $H_{c2}(0) = 16.3 \text{ T}$  was estimated for the powder sample, in which  $T_c$  was defined at the middle point of the transition.<sup>13</sup>

In Fig. 1b, the normalized ac magnetization for  $\text{FeSe}_x$  single crystal is plotted. The positive ferromagnetic background has been attributed to the existence of Fe impurity in the  $\text{FeSe}_x$  powder sample.<sup>13</sup> However, no iron, iron oxide, or iron silicide impurities were detected in our crystals,<sup>21</sup> therefore the ferromagnetic background likely results from the magnetic Fe cluster promoted by Se vacancies.<sup>29</sup>

Fig. 2 shows the temperature dependence of the in-plane thermal conductivity for  $\text{FeSe}_x$  in zero field. To extrapolate the residual linear term  $\kappa_0/T$ , we fit the data to  $\kappa/T = a + bT^{\alpha-1}$ ,<sup>30,31</sup> where  $aT$  and  $bT^{\alpha}$  represent electronic and phonon contributions, respectively. In Fig. 2, the data from 120 mK to 0.7 K can be fitted (the solid line) and gives  $\kappa_0/T = 16 \pm 2 \mu\text{W K}^{-2} \text{ cm}^{-1}$ , with  $\alpha = 2.47$ .

Such a value of  $\kappa_0/T$  is slightly larger than the experimental error bar  $\pm 5 \mu\text{W K}^{-2} \text{ cm}^{-1}$ .<sup>31</sup> However, it is still fairly small, less than 4% the normal state Wiedemann-Franz law expectation  $\kappa_{N0}/T = L_0/\rho_0 = 0.423 \text{ mW K}^{-2} \text{ cm}^{-1}$ , with  $L_0$  the Lorenz number  $2.45 \times 10^{-8} \text{ W } \Omega \text{ K}^{-2}$  and  $\rho_0 = 57.9 \mu\Omega \text{ cm}$ . For unconventional superconductors with nodes in the superconducting gap, a substantial  $\kappa_0/T$  in zero field contributed by the nodal quasiparticles has been found.<sup>32,33</sup> For example, for overdoped  $d$ -wave cuprate superconductor  $\text{Tl}2201$  with  $T_c = 15 \text{ K}$ ,  $\kappa_0/T = 1.41 \text{ mW K}^{-2} \text{ cm}^{-1}$ , about 36%  $\kappa_{N0}/T$ .<sup>32</sup> For  $p$ -wave superconductor  $\text{Sr}_2\text{RuO}_4$  with  $T_c = 1.5 \text{ K}$ ,  $\kappa_0/T$

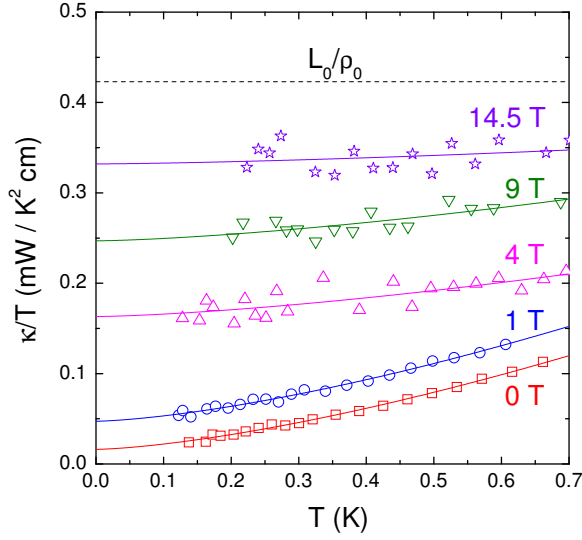


FIG. 3: (Color online) Low-temperature thermal conductivity of  $\text{FeSe}_x$  in magnetic fields applied along the  $c$ -axis ( $H = 0, 1, 4, 9$ , and  $14.5$  T). The solid lines are  $\kappa/T = a + bT^{\alpha-1}$  fits. For  $H = 4, 9$ , and  $14.5$  T, the electronic contribution becomes more and more dominant and the data get less smooth, therefore  $\alpha$  is fixed to 2.47. The dashed line is the normal state Wiedemann-Franz law expectation at  $T \rightarrow 0$ , namely  $L_0/\rho_0$ , with  $L_0$  the Lorenz number  $2.45 \times 10^{-8} \text{ W } \Omega \text{ K}^{-2}$ .

$= 17 \text{ mW K}^{-2} \text{ cm}^{-1}$ , more than 9%  $\kappa_{N0}/T$  for the best sample.<sup>33</sup> We also note that  $\kappa_0/T$  in zero field are all negligible in closely related superconductors  $\text{BaNi}_2\text{As}_2$ ,  $\text{Ba}_{1-x}\text{K}_x\text{Fe}_2\text{As}_2$ , and  $\text{BaFe}_{1.9}\text{Ni}_{0.1}\text{As}_2$ .<sup>24,25,26</sup> Therefore, it is unlikely that  $\kappa_0/T = 16 \pm 2 \mu\text{W K}^{-2} \text{ cm}^{-1}$  in  $\text{FeSe}_x$  single crystal comes from the nodal quasiparticles. Since no impurity phases were detected, such a small  $\kappa_0/T$  may simply come from the slight overestimation when doing extrapolation, due to the lack of experimental data below 120 mK.

Below we turn to the field dependence of  $\kappa_0/T$  in  $\text{FeSe}_x$ . Fig. 3 shows the low-temperature thermal conductivity of  $\text{FeSe}_x$  in magnetic fields applied along the  $c$ -axis ( $H = 0, 1, 4, 9$ , and  $14.5$  T). For  $H = 1$  T, the data is also fitted to  $\kappa/T = a + bT^{\alpha-1}$ , and gives  $\kappa_0/T = 47 \pm 2 \mu\text{W K}^{-2} \text{ cm}^{-1}$ , with  $\alpha = 2.47$ . For  $H = 4, 9$ , and  $14.5$  T, the electronic contribution becomes more and more dominant and the data get less smooth, therefore  $\alpha$  is fixed to 2.47 in the phonon term  $bT^\alpha$ . From Fig. 3, even higher magnetic field is needed to increase  $\kappa/T$  to its normal state value.

In Fig. 4, we put the normalized  $\kappa_0/T(H)$  of  $\text{FeSe}_x$  together with the clean  $s$ -wave superconductor Nb,<sup>34</sup> the dirty  $s$ -wave superconducting alloy InBi,<sup>35</sup> the multi-band  $s$ -wave superconductor NbSe<sub>2</sub><sup>36</sup> and an overdoped sample of the  $d$ -wave superconductor Tl-2201,<sup>32</sup> plotted as a function of  $H/H_{c2}$ . For a clean (like Nb) or dirty (like InBi) type-II  $s$ -wave superconductor with isotropic gap,  $\kappa_0/T$  should grow exponentially with field (above  $H_{c1}$ ). This usually gives negligible  $\kappa_0/T$  for field lower than

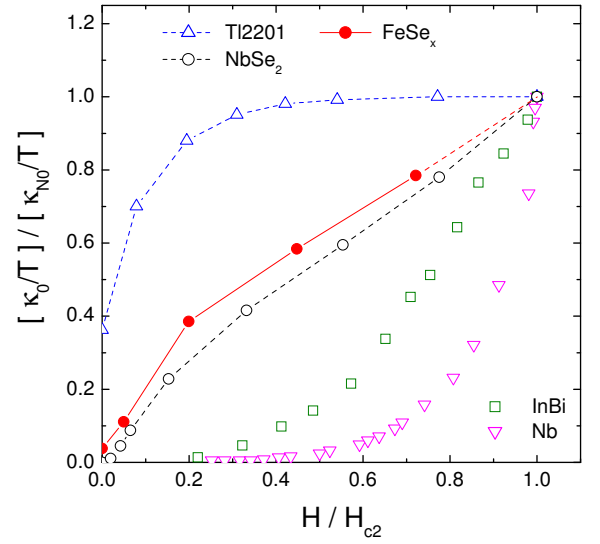


FIG. 4: (Color online) Normalized residual linear term  $\kappa_0/T$  of  $\text{FeSe}_x$  plotted as a function of  $H/H_{c2}$ . Similar data of the clean  $s$ -wave superconductor Nb,<sup>34</sup> the dirty  $s$ -wave superconducting alloy InBi,<sup>35</sup> the multi-band  $s$ -wave superconductor NbSe<sub>2</sub>,<sup>36</sup> and an overdoped sample of the  $d$ -wave superconductor Tl-2201<sup>32</sup> are also shown for comparison.

$H_{c2}/4$ . For the  $d$ -wave superconductor Tl-2201,  $\kappa_0/T$  increases roughly proportional to  $\sqrt{H}$  at low field due to the Volovik effect.<sup>37</sup> By contrast, for multi-gap superconductors NbSe<sub>2</sub> and MgB<sub>2</sub>,<sup>36,38</sup> magnetic field will first suppress the superconductivity on the Fermi surface with smaller gap, and give distinct shape of  $\kappa_0/T(H)$  curve, as seen in Fig. 4.

From Fig. 4, the  $\kappa_0/T(H)$  of  $\text{FeSe}_x$  manifests almost identical behavior as that of multi-gap  $s$ -wave superconductor NbSe<sub>2</sub>. For NbSe<sub>2</sub>, the shape of  $\kappa_0/T(H)$  has been quantitatively explained by multiband superconductivity, whereby the gap on the  $\Gamma$  band is approximately one third of the gap on the other two Fermi surfaces.<sup>36</sup> Therefore, we consider our data as strong evidence for multi-gap nodeless superconductivity in  $\text{FeSe}_x$ . Note that in the two-gap  $s + s$ -wave model to describe the in-plane penetration depth data, the magnitude of the two gaps are 1.60 and 0.38 meV, respectively.<sup>22</sup> The ratio between these two gaps is about 4, close to that in NbSe<sub>2</sub>, thus supports the multi-gap scenario from our thermal conductivity results.

So far, there is still no experiment to directly measure the superconducting gap in  $\text{Fe}_{1+y}\text{Te}_{1-x}\text{Se}_x$  system. Density functional calculations show that the electronic band structure of FeS, FeSe, and FeTe are very similar to the FeAs-based superconductors.<sup>39</sup> In doped  $\text{BaFe}_2\text{As}_2$ , multi-gap nodeless superconductivity has been clearly demonstrated by angle-resolved photoemission spectroscopy (ARPES) experiments.<sup>40,41,42</sup> For hole-doped  $\text{Ba}_{0.6}\text{K}_{0.4}\text{Fe}_2\text{As}_2$  ( $T_c = 37$  K), the average gap values  $\Delta(0)$  for the two hole pockets ( $\alpha$  and  $\beta$ ) are 12.5 and 5.5 meV, respectively, while for the electron ( $\gamma$  and

$\delta$ ) pockets, the gap value is similar, about 12.5 meV.<sup>40,41</sup> For electron-doped  $\text{BaFe}_{1.85}\text{Co}_{0.15}\text{As}_2$  ( $T_c = 25.5$  K), the average gap values  $\Delta(0)$  of hole ( $\beta$ ) and electron ( $\gamma$  and  $\delta$ ) pockets are 6.6 and 5.0 meV, respectively<sup>42</sup>. The ratio between the large and small gaps is 2.3 for  $\text{Ba}_{0.6}\text{K}_{0.4}\text{Fe}_2\text{As}_2$ . This may explain the rapid increase of  $\kappa_0/T(H)$  at low field in  $\text{Ba}_{1-x}\text{K}_x\text{Fe}_2\text{As}_2$ ,<sup>25</sup> although magnetic field was only applied up to  $1/4 H_{c2}$  thus could not see clear multi-gap character as in our  $\text{FeSe}_x$  single crystal.

In summary, we have measured the low-temperature thermal conductivity of iron selenide superconductor  $\text{FeSe}_x$  to investigate its superconducting gap structure. A fairly small  $\kappa_0/T$  at zero field and the dramatic field dependence of  $\kappa_0/T$  give strong evidence for multi-gap nodeless superconductivity in  $\text{FeSe}_x$ . Such a gap struc-

ture may be generic for all Fe-based superconductors. More experiments are needed to distinguish conventional  $s$ -wave from the unconventional  $s^\pm$ -wave superconductivity in this new family of high- $T_c$  superconductors.

This work is supported by the Natural Science Foundation of China, the Ministry of Science and Technology of China (National Basic Research Program No:2009CB929203), Program for New Century Excellent Talents in University, and STCSM of China (No: 08dj1400200 and 08PJ1402100). The work in Northern Illinois University was supported by the US Department of Energy Grant No. DE-FG02-06ER46334 and Contract No. DE-AC02-06CH11357.

\* E-mail: shiyan\_li@fudan.edu.cn

- <sup>1</sup> Y. Kamihara, T. Watanabe, M. Hirano, and H. Hosono, *J. Am. Chem. Soc.* **130**, 3296 (2008).
- <sup>2</sup> X. H. Chen, T. Wu, G. Wu, R. H. Liu, H. Chen, and D. F. Fang, *Nature* **453**, 761 (2008).
- <sup>3</sup> G. F. Chen, Z. Li, D. Wu, G. Li, W. Z. Hu, J. Dong, P. Zheng, J. L. Luo, and N. L. Wang, *Phys. Rev. Lett.* **100**, 247002 (2008).
- <sup>4</sup> Zhi-An Ren, Wei Lu, Jie Yang, Wei Yi, Xiao-Li Shen, Zheng-Cai Li, Guang-Can Che, Xiao-Li Dong, Li-Ling Sun, Fang Zhou, and Zhong-Xian Zhao, *Chin. Phys. Lett.* **25**, 2215 (2008).
- <sup>5</sup> R. H. Liu, G. Wu, T. Wu, D. F. Fang, H. Chen, S. Y. Li, K. Liu, Y. L. Xie, X. F. Wang, R. L. Yang, C. He, D. L. Feng, and X. H. Chen, *Phys. Rev. Lett.* **101**, 087001 (2008).
- <sup>6</sup> M. Rotter, M. Tegel, and D. Johrendt, *Phys. Rev. Lett.* **101**, 107006 (2008).
- <sup>7</sup> X. C. Wang, Q. Q. Liu, Y. X. Lv, W. B. Gao, L. X. Yang, R. C. Yu, F. Y. Li, and C. Q. Jin, *Solid State Commun.* **148**, 538 (2008).
- <sup>8</sup> A. S. Sefat, A. Huq, M. A. McGuire, R. Jin, B. C. Sales, D. Mandrus, *Phys. Rev. B* **78**, 104505 (2008).
- <sup>9</sup> Guanghan Cao, Shuai Jiang, Xiao Lin, Cao Wang, Yuke Li, Zhi Ren, Qian Tao, Jianhui Dai, Zhu'an Xu, Fu-Chun Zhang, *Phys. Rev. B* **79**, 174505 (2009).
- <sup>10</sup> A. S. Sefat R. Jin, M. A. McGuire, B. C. Sales, D. J. Singh, D. Mandrus, *Phys. Rev. Lett.* **101**, 117004 (2008).
- <sup>11</sup> L. J. Li, Q. B. Wang, Y. K. Luo, H. Chen, Q. Tao, Y. K. Li, X. Lin, M. He, Z. W. Zhu, G. H. Cao, Z. A. Xu, *New J. Phys.* **11**, 025008 (2009).
- <sup>12</sup> Shuai Jiang, Cao Wang, Zhi Ren, Yongkang Luo, Guanghan Cao, and Zhu'an Xu, arXiv:0901.3227.
- <sup>13</sup> Fong-Chi Hsu, Jiu-Yong Luo, Kuo-Wei Yeh, Ta-Kun Chen, Tzu-Wen Huang, Phillip M. Wu, Yong-Chi Lee, Yi-Lin Huang, Yan-Yi Chu, Der-Chung Yan, and Maw-Kuen Wu, *Proc. Natl. Acad. Sci. USA* **105**, 14262 (2008).
- <sup>14</sup> Y. Mizuguchi, F. Tomioka, S. Tsuda, T. Yamaguchi, and Y. Takano, *Appl. Phys. Lett.* **93**, 152505 (2008).
- <sup>15</sup> S. Medvedev, T. M. McQueen, I. A. Troyan, T. Palasyuk, M. I. Erements, R. J. Cava, S. Naghavi, F. Casper, V. Ksenofontov, G. Wortmann, and C. Felser *Nature Mater.* doi:10.1038/NMAT2491 (2009)
- <sup>16</sup> S. Margadonna, Y. Takabayashi, Y. Ohishi, Y. Mizuguchi, Y. Takano, T. Kagayama, T. Nakagawa, M. Takata, and K. Prassides, arXiv:0903.2204.
- <sup>17</sup> I. I. Mazin and J. Schmalian, arXiv:0901.4790.
- <sup>18</sup> K. Ishida, Y. Nakai, and H. Hosono, arXiv:0906.2405.
- <sup>19</sup> I. I. Mazin, D. J. Singh, M. D. Johannes, and M. H. Du, *Phys. Rev. Lett.* **101**, 057003 (2008).
- <sup>20</sup> S. B. Zhang, Y. P. Sun, X. D. Zhu, X. B. Zhu, B. S. Wang, G. Li, H. C. Lei, X. Luo, Z. R. Yang, W. H. Song, and J. M. Dai, *Supercond. Sci. Technol.* **22**, 015020 (2009).
- <sup>21</sup> U. Patel, J. Hua, S. H. Yu, S. Avci, Z. L. Xiao, H. Claus, J. Schlueter, V. V. Vlasko-Vlasov, U. Welp, and W. K. Kwok, *Appl. Phys. Lett.* **94**, 082508 (2009).
- <sup>22</sup> R. Khasanov, K. Conder, E. Pomjakushina, A. Amato, C. Baines, Z. Bukowski, J. Karpinski, S. Katrych, H.-H. Klauss, H. Luetkens, A. Shengelaya, and N. D. Zhigadlo, *Phys. Rev. B* **78**, 220510(R) (2008).
- <sup>23</sup> H. Shakeripour, C. Petrovic, Louis Taillefer, *New Journal of Physics* **11**, 055065 (2009).
- <sup>24</sup> N. Kurita, F. Ronning, Y. Tokiwa, E. D. Bauer, A. Subedi, D. J. Singh, J. D. Thompson, and R. Movshovich, *Phys. Rev. Lett.* **102**, 147004 (2009).
- <sup>25</sup> X. G. Luo, M. A. Tanatar, J.-Ph. Reid, H. Shakeripour, N. Doiron-Leyraud, N. Ni, S. L. Bud'ko, P. C. Canfield, Huiqian Luo, Zhaosheng Wang, Hai-Hu Wen, Ruslan Prozorov, and Louis Taillefer, arXiv:0904.4049.
- <sup>26</sup> L. Ding, J. K. Dong, S. Y. Zhou, T. Y. Guan, X. Qiu, C. Zhang, L. J. Li, X. Lin, G. H. Cao, Z. A. Xu, and S. Y. Li, arXiv:0906.0138.
- <sup>27</sup> T. M. McQueen, Q. Huang, V. Ksenofontov, C. Felser, Q. Xu, H. Zandbergen, Y. S. Hor, J. Allred, A. J. Williams, D. Qu, J. Checkelsky, N. P. Ong, and R. J. Cava, *Phys. Rev. B* **79**, 014522 (2009).
- <sup>28</sup> E. Pomjakushina, K. Conder, V. Pomjakushin, M. Bendele, and R. Khasanov, arXiv:0905.2115.
- <sup>29</sup> K. W. Lee, V. Pardo, and W. E. Pickett, *Phys. Rev. B* **78**, 174502 (2008).
- <sup>30</sup> M. Sutherland, D. G. Hawthorn, R. W. Hill, F. Ronning, S. Wakimoto, H. Zhang, C. Proust, Etienne Boaknin, C. Lupien, Louis Taillefer, Ruixing Liang, D. A. Bonn, W. N. Hardy, Robert Gagnon, N. E. Hussey, T. Kimura, M. Nohara, and H. Takagi, *Phys. Rev. B* **67**, 174520 (2003).
- <sup>31</sup> S. Y. Li, J.-B. Bonnemaïson, A. Payeur, P. Fournier, C. H.

- Wang, X. H. Chen, and Louis Taillefer, Phys. Rev. B **77**, 134501 (2008).
- <sup>32</sup> C. Proust, E. Boaknin, R. W. Hill, L. Taillefer, and A. P. Mackenzie, Phys. Rev. Lett. **89**, 147003 (2002).
- <sup>33</sup> M. Suzuki, M. A. Tanatar, N. Kikugawa, Z. Q. Mao, Y. Maeno, and T. Ishiguro, Phys. Rev. Lett. **88**, 227004 (2002).
- <sup>34</sup> J. Lowell and J. Sousa, J. Low. Temp. Phys. **3**, 65 (1970).
- <sup>35</sup> J. Willis and D. Ginsberg, Phys. Rev. B **14**, 1916 (1976).
- <sup>36</sup> E. Boaknin, M. A. Tanatar, Johnpierre Paglione, D. Hawthorn, F. Ronning, R. W. Hill, M. Sutherland, Louis Taillefer, Jeff Sonier, S. M. Hayden, and J. W. Brill, Phys. Rev. Lett. **90**, 117003 (2003).
- <sup>37</sup> G. E. Volovik, JETP Lett. **58**, 469 (1993).
- <sup>38</sup> A. V. Sologubenko, J. Jun, S. M. Kazakov, J. Karpinski, and H. R. Ott, Phys. Rev. B **66**, 014504 (2002).
- <sup>39</sup> Alaska Subedi, Lijun Zhang, D. J. Singh, and M. H. Du, Phys. Rev. B **78**, 134514 (2008).
- <sup>40</sup> H. Ding, P. Richard, K. Nakayama, T. Sugawara, T. Arakane, Y. Sekiba, A. Takayama, S. Souma, T. Sato, T. Takahashi, Z. Wang, X. Dai, Z. Fang, G. F. Chen, J. L. Luo, N. L. Wang, Europhys. Lett. **83** 47001 (2008).
- <sup>41</sup> K. Nakayama, T. Sato, P. Richard, Y.-M. Xu, Y. Sekiba, S. Souma, G. F. Chen, J. L. Luo, N. L. Wang, H. Ding, and T. Takahashi, arXiv:0812.0663.
- <sup>42</sup> K. Terashima, Y. Sekiba, J. H. Bowen, K. Nakayama, T. Kawahara, T. Sato, P. Richard, Y.-M. Xu, L. J. Li, G. H. Cao, Z.-A. Xu, H. Ding, and T. Takahashi, arXiv:0812.3704.